

ChemComm

Chemical Communications

Accepted Manuscript

This article can be cited before page numbers have been issued, to do this please use: M. Van Hoof, L. Bynens, B. Daelemans, M. C. Rodriguez Gonzalez, L. Van Meervelt, S. De Feyter and W. Dehaen, *Chem. Commun.*, 2022, DOI: 10.1039/D2CC02070J.



This is an Accepted Manuscript, which has been through the Royal Society of Chemistry peer review process and has been accepted for publication.

Accepted Manuscripts are published online shortly after acceptance, before technical editing, formatting and proof reading. Using this free service, authors can make their results available to the community, in citable form, before we publish the edited article. We will replace this Accepted Manuscript with the edited and formatted Advance Article as soon as it is available.

You can find more information about Accepted Manuscripts in the [Information for Authors](#).

Please note that technical editing may introduce minor changes to the text and/or graphics, which may alter content. The journal's standard [Terms & Conditions](#) and the [Ethical guidelines](#) still apply. In no event shall the Royal Society of Chemistry be held responsible for any errors or omissions in this Accepted Manuscript or any consequences arising from the use of any information it contains.

COMMUNICATION

Octahydropyrimido[4,5-g]quinazoline-5,10-diones: Their multicomponent synthesis, self-assembly on graphite and electrochemistry

Received 00th January 20xx,
Accepted 00th January 20xx

DOI: 10.1039/x0xx00000x

Max Van Hoof,^a Lize Bynens,^b Brent Daelemans,^c Miriam Candelaria Rodríguez González,^c Luc Van Meervelt,^d Steven De Feyter,^c Wim Dehaen^{*a}

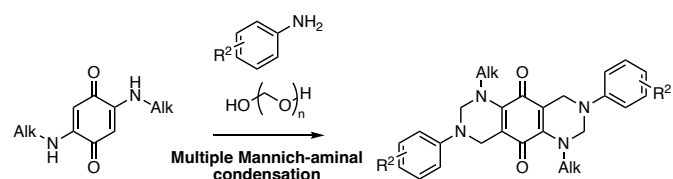
A green multicomponent synthesis of previously unreported octahydropyrimido[4,5-g]quinazoline-5,6-diones was developed from simple building blocks. These highly symmetrical compounds show strong propensity to self-assembled molecular network (SAMN) formation on highly oriented pyrolytic graphite. The SAMN type is easily tunable by changing molecular characteristics. The redox behavior was studied by cyclic voltammetry.

Quinones are a class of redox-active molecules that are represented widely in nature, where they function in a variety of vital electron-transport processes including photosynthesis and respiration.^{1,2} Their unique properties give rise to a broad range of bioactivities including in anticancer, antifungal, antibacterial and antiparasitic drugs.^{3–6} Additionally, quinones have found many applications in energy-harvesting and storage materials, for example in Li-ion batteries and pseudocapacitors.⁷ One persistent issue with these quinone-based materials is their dissolution into electrolytes which limits the recyclability of these materials. A possible solution could be to immobilize the quinones using molecular self-assembly on a conducting carbon-based nanomaterial such as graphene or graphite.^{7,8}

A particularly interesting class of quinone compounds are 2,5-diaminoquinones, due to their straightforward synthesis, interesting reactivity, and self-assembly behavior. While it is known that zwitterionic *m*-diaminobenzoquinones form self-assembled molecular networks (SAMNs) on graphite via strong charge-assisted hydrogen bonding,¹¹ the self-assembly of *p*-diaminobenzoquinones is far less investigated. The only reported strategy is the self-assembly of a *p*-diaminobenzoquinone containing two long alkyl chains that forms SAMNs stabilized by π - π interactions between the

aryl group and graphite and by Van der Waals (VDW) interactions between the long alkyl chains and the surface, and between adjacent alkyl chains.¹² For these compounds the only modifiable groups are the alkyl chains, restricting the scope of 2D crystal engineering. Additional design positions would be beneficial for optimizing the control over SAMN formation, as well as other materials' properties.

In this work, the enamine reactivity of *p*-dialkylaminobenzoquinones was exploited in a multiple Mannich-aminal condensation, affording 1,2,3,4,6,7,8-octahydropyrimido[4,5-g]quinazolin-5,10-diones (Scheme 1). In contrast to the previously reported *p*-diaminobenzoquinones, these compounds have four groups on the nitrogen atoms that can be easily varied, the alkyl and the aryl substituents, enabling straightforward design of the different stabilizing interactions for SAMN formation. The pyrimido[4,5-g]quinazolin-5,10-diones with short alkyl chains do not have the strong VDW stabilization of long alkyl chains that could favor the formation of SAMNs. Nevertheless, they show a high tendency towards dense and close-packed SAMN formation on graphite, via parallel displaced π -stacking of the anilines. When transitioning to long alkyl chain substituents on the pyrimido[4,5-g]quinazolin-5,10-diones a less dense structure is formed as VDW interactions again become dominant.



Scheme 1. The multiple Mannich-aminal condensation of 2,5-diamino-*p*-benzoquinones allows straightforward access to SAMN forming pyrimido[4,5-g]quinazolin-5,10-diones

Inspired by the synthesis of 1,2,3,4-tetrahydrobenzo[*g*]quinazolin-5,10-diones from naphthoquinone derivatives,^{13–15} and by the many Mannich-aminal condensations of enaminones towards tetrahydropyrimidines,^{16–21} the reaction of *p*-dialkylaminoquinones towards octahydropyrimido[4,5-g]quinazolin-5,10-diones was optimized. To the best of our knowledge, octahydropyrimido[4,5-g]quinazolin-5,10-diones have not been previously described. The developed multicomponent reaction, with seven reaction partners,

^a Molecular Design and Synthesis, Department of Chemistry, KU Leuven, Celestijnenlaan 200F, B-3001 Leuven, Belgium. Email: Wim Dehaen (W. Dehaen). Email: wim.dehaen@kuleuven.be

^b Hasselt University, Institute for Materials Research (IMO), Agoralaan Building D, 3590, Diepenbeek, Belgium

^c Division of Molecular Imaging and Photonics, Department of Chemistry, KU Leuven, Celestijnenlaan 200F, 3001 Leuven, Belgium. E-mail: steven.defeyter@kuleuven.be

^d Biomolecular Architecture, Department of Chemistry, KU Leuven Celestijnenlaan 200F, Leuven B-3001, Belgium. E-mail: luc.vanmeervelt@kuleuven.be
Electronic Supplementary Information (ESI) available: [details of any supplementary information available should be included here]. See DOI: 10.1039/x0xx00000x

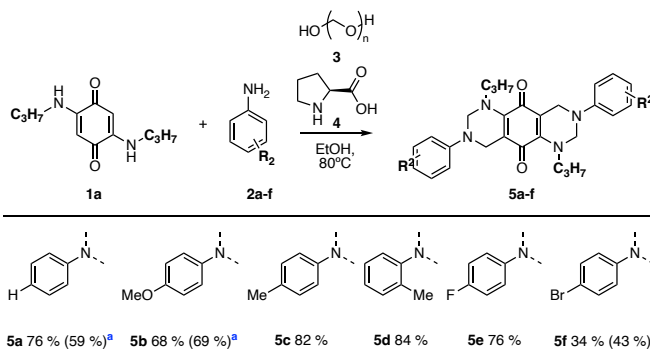
allows simultaneous incorporation of six components onto the *p*-diaminobenzoquinone core in a single step, using readily available starting materials. Notably, this reaction is of minimal environmental impact for two reasons. Firstly, ethanol and L-proline are used as respectively green solvent and green organocatalyst. Secondly, the reaction products are generally isolated via simple filtration. Therefore, the reaction proved to be easily scalable, and could be applied to gram-scale synthesis.

Under the optimized conditions (Scheme 2, for more details consult Supp. Info section '1.3 Optimization studies', pages S6 – S7), 2,5-di(propylamino)benzoquinone **1a** was reacted at 80 °C with 2 equivalents of aniline **2a**, twofold excess (8 equivalents) of paraformaldehyde **3**, and 1 equivalent of proline **4** in ethanol (0.5 M). The final compound **5a** precipitated from the reaction mixture and could be obtained in 76 % yield *via* simple filtration. The reaction with *p*-anisidine **2b** afforded compound **5b** in 68 % yield. Pleasingly, the cyclized products from both *o*- and *p*-toluidine **5c** and **5d** could be obtained in similar yields of 82 % (**5c**) and 84 % (**5d**), indicating that also more sterically hindered anilines are successful. Also, 4-fluoro- and 4-bromo-substituted **5e** and **5f** could be obtained in 76 % (**5e**) and 34 % (**5f**) yield, showing that weakly withdrawing groups are tolerated. The lower yield of 4-bromoaniline **5f** compared to 4-fluoroaniline **5e** presumably results from two reasons. Firstly, the nucleophilicity of 4-bromoaniline **2f** is slightly lower than 4-fluoroaniline **2e**, when comparing their Hammett constants σ_p of 0.23 and 0.06.²² Secondly, the solubility of bromo-substituted **5f** is greater than fluoro-substituted **5e** which may hinder product precipitation as thermodynamic driving force. Indeed, in the reaction towards **5f** the onset of product precipitation occurred comparatively late. As expected, the reaction is unsuccessful when poorly nucleophilic anilines, substituted with (strongly) withdrawing groups, are used which is in line with the limitations for the somewhat analogous Tröger's base synthesis.²³ No product could be isolated from the reactions of ethyl-4-aminobenzoate, 4-aminobenzonitrile, 4-(trifluoromethyl)aniline and 4-nitroaniline. At this point, the gram-scale synthesis was attempted using aniline **2a**, *p*-anisidine **2b** and 4-bromoaniline **2f** which gave comparable yields of 59 % (**5a**), 69 % (**5b**) and 43 % (**5f**), clearly showing that the reaction is scalable.

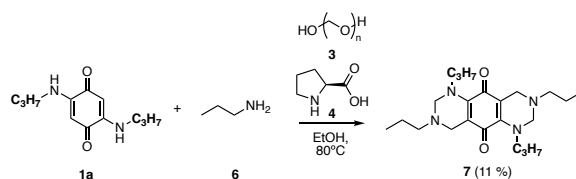
Finally, the reaction of **1a** with propylamine and formaldehyde gave compound **7** in a reduced yield of 11 %, presumably due to increased solubility of **6** and decreased stability of the formed aliphatic tertiary amine under the reaction conditions (Scheme 3). Next, the scope was evaluated using various di(substituted amino)quinones **1b-d** with both aniline **2a** and 4-bromoaniline **2f** (Scheme 4). The reaction of dimethylaminoquinone **1b** gave compound **8a** and **8b** in 65 % and 50 % yield, both isolated by filtration. Dihexaminoquinone **1c** gave **9a** isolated via filtration in 62 % yield and **9b** isolated by flash chromatography in 29 % yield. For compound **9a** the structure was confirmed by single-crystal X-ray diffraction (for more details see Supp. Info section '1.6. Crystal structure determination of 9a', pages S17 – S20). Didodecylaminoquinone **1d** gave compounds **10a** isolated via filtration in 75 % isolated yield, and **10b** isolated via flash chromatography in 37 % yield. However, the reactions of 2,5-dibenzylaminoquinone or 2,5-diphenylaminoquinone were

unsuccessful, and no conversion was observed due to their very low solubility in ethanol.

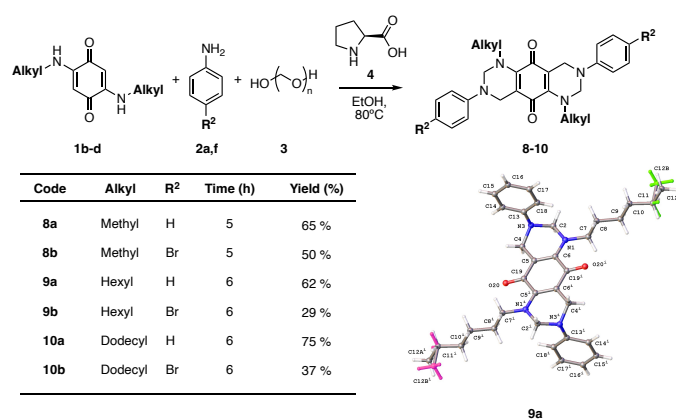
DOI: 10.1039/D2CC02070J



Scheme 2. Substrate scope for anilines. Reaction conditions: **1** (0.5 mmol), aniline **2** (1.0 mmol), paraformaldehyde **3** (4.00 mmol), L-proline **4** (0.5 mmol), EtOH (1 mL), 80°C, 5h. Isolated yields. ^aYields from gram-scale experiment.



Scheme 3. Evaluation of aliphatic amine. Reaction conditions: **1** (5 mmol), *n*-propylamine **6** (10 mmol), paraformaldehyde **3** (40 mmol), L-proline **4** (5 mmol), EtOH (30 mL), 80°C, 2h30. Isolated yield.



Scheme 4. Reaction of dialkylaminoquinones **1b-d** with unsubstituted and 4-bromoanilines **2a** and **2f**. Reaction conditions: **1** (0.5 mmol), aniline **2** (1.0 mmol), paraformaldehyde **3** (4.00 mmol), L-proline **4** (0.5 mmol), EtOH (1 mL), 80°C, 5h. Isolated yields. Single crystal X-ray structure for compound **9a**.

The on-surface behavior of the different pyrimido[4,5-*g*]quinazolin-5,10-diones was investigated using high-resolution scanning tunnelling microscopy (STM) experiments. STM allows visualization of SAMN formation at the liquid/solid interface. To determine the effect of the molecular structure on the formed SAMNs, both the functional group on the aniline and the length of the alkyl chain were varied. Solutions of 0.5 mM were made in 1-phenyloctane (1-PO) which is a common solvent in STM experiments. This solvent was chosen because of its low vapor pressure, electrochemical inertness, and non-acidic behavior. The solution was drop-casted on a freshly

cleaved highly oriented pyrolytic graphite (HOPG) surface and the SAMN was visualized at the liquid/solid interface.

The first attempted variation included compounds derived from anilines with variable functional groups. Four different aniline derivatives were evaluated for determining their effect on SAMN formation on the HOPG surface: i) aniline **5a**, ii) 4-methylaniline **5c**, iii) 4-fluoroaniline **5e**, and iv) 4-bromoaniline **5f**. For compound **5a**, which contains two aniline moieties, no SAMN formation was observed on HOPG. The other compounds, containing two 4-methylaniline (**5c**), two 4-fluoroaniline (**5e**) or two 4-bromoaniline moieties (**5f**), were observed to form a close-packed self-assembled structure at the liquid/solid interface (Figure 1). The models indicate stabilization by π - π interactions between the quinone moiety and the graphite surface. While similar π - π interactions could be expected for the aniline groups at the outside of the molecules, these groups were observed to self-assemble edge-on to the surface to enhance π - π interactions between adjacent aniline groups in a parallel displaced stacking. The edge-on orientation on the surface has been reported for molecules containing largely conjugated systems, such as porphyrins,²⁴ or other strong directional intermolecular interactions, such as hydrogen bonding.²⁵ However, the results obtained from these experiments show that a parallel displaced stacking of substituted aniline groups can be sufficient to act as directional intermolecular interactions in the SAMN and convert the aniline groups to an edge on-orientation. Compounds **5c** (methyl), **5e** (fluoro), and **5f** (bromo) are observed to assemble in similar SAMNs where the difference in unit cell can be explained by the difference in size and electrostatic interactions between the methyl, the fluoro and the bromo group. The absence of SAMN formation for compound **5a** with two aniline moieties can be explained by enhanced π - π interactions of substituted aryl groups, which are absent for the aniline moieties in **5a**.^{26,27} The second set of experiments focuses on the effect of the alkyl chain length on the SAMN formation on the surface, specifically by increasing the alkyl chain length of the compound with 4-bromoaniline groups from propyl (**5f**) to hexyl (**9b**) and dodecyl (**10b**) substituents. The molecules containing propyl chains, as discussed previously, self-assemble in close-packed structures. When the chain length is increased to hexyl, no formation of a self-assembled structure on the surface is observed. This absence of a SAMN for compound **9b** can be explained by increased steric hindrance of the hexyl chains, which inhibits formation of the close-packed self-assembled structure. Increasing the chain length to a dodecyl chain (**10b**) enables again the formation of a SAMN, however, the packing of molecules on the surface changed significantly. According to our proposed models, the close-packed structure for propyl compound **5f** is altered to a less dense structure when going to dodecyl chains in **10b**. This structure with extended alkyl chains favors interdigitation of the alkyl chains that increase the VDW interactions and stabilize the SAMN.

Quinone-containing compounds are known to show a reversible response in cyclic voltammetry under aqueous conditions.²⁸ However, considering that the octahydropyrimido[4,5-*g*]quinazolin-5,10-diones prepared in this work are poorly soluble in water, dimethylformamide (DMF) was selected as solvent for establishing the differences in redox behavior of these compounds. In general, in

non-aqueous electrolytes the electrochemical behavior of these molecules is far more complex compared to aqueous conditions. The analysis of the different processes is not straightforward, involving in most cases quasi-reversible and irreversible redox reactions.²⁹ For instance, the electrochemical response of isolapachol was studied in DMF, showing electrochemical behavior with the occurrence of self-protonation or hydrogen bonding intermediate formation.³⁰ Nevertheless, shifts in the potential for these voltametric features can be used to indicate different reactivity of the compounds, and gives valuable information.

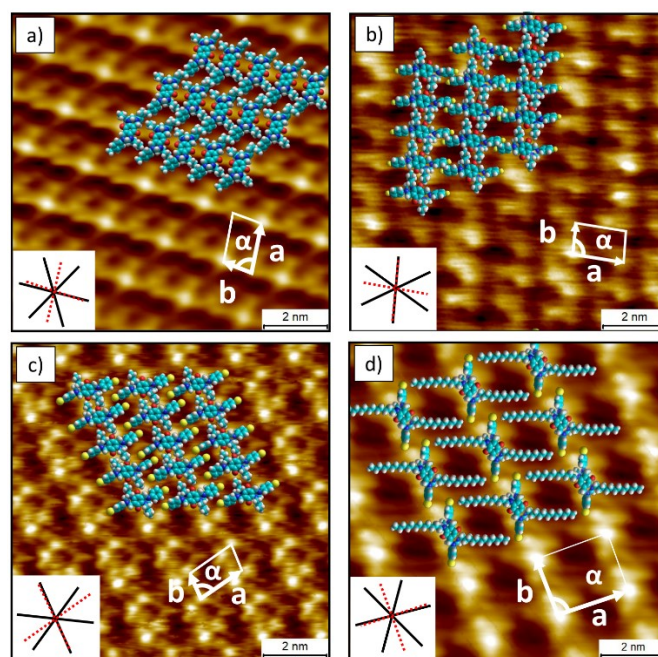


Figure 1. STM images at the liquid/solid interface, including the proposed models, the unit cells (white), where a and b are the unit cell vectors and α is the unit cell angle, and the inset, where the graphite symmetry axes (black lines) are compared to the unit cell vectors (red dotted lines). a) Compound **5c** (methyl), unit cell (Plane group $p2$, 1 molecule): a : 1.52 ± 0.01 nm, b : 0.98 ± 0.01 nm, α : $85.0 \pm 0.8^\circ$, b) Compound **5e** (Fluoro), unit cell (Plane group $p2$, 1 molecule): a : 1.65 ± 0.06 nm, b : 0.96 ± 0.02 nm, α : $86 \pm 3^\circ$, c) Compound **5f** (Bromo), unit cell (Plane group $p2$, 1 molecule): a : 1.74 ± 0.07 nm, b : 1.01 ± 0.03 nm, α : $81 \pm 4^\circ$, and d) Compound **10b** (C12), unit cell (Plane group $p2$, 1 molecule): a : 2.27 ± 0.04 nm, b : 2.02 ± 0.04 nm, α : $91 \pm 3^\circ$. On these figures, the proposed models and the unit cells (white) are indicated. Imaging conditions: 0.5 mM in 1-PO, $I_{set} = 0.020$ - 0.050 nA, $V_{bias} = -0.800$ - -0.500 V.

Figure S2 (Supp. Info page 22) shows the cyclic voltammogram for the dipropylaminoquinone **1a** and several of the octahydropyrimido[4,5-*g*]quinazolin-5,10-diones. All tested compounds show characteristic oxidation and reduction peaks relative to the blank (bare HOPG, black line). The aminoquinone **1a** oxidation occurs around 1.5 V (pink line), which clearly differs with respect to the octahydropyrimido[4,5-*g*]quinazolin-5,10-diones, whose oxidation occurs close to 1 V. However, this oxidation is comparatively shifted towards less positive potentials in the case of the aniline derived compound **5a**, *p*-anisidine compound **5b** and *p*-toluidine compound **5c**. For all compounds at least three redox couples with a large irreversibility can be seen. A reversible couple is found in several cases around 0.25V, which is especially clearly visible in the case of the dodecylamino compound **10a**.

Conclusions

In conclusion, an environmentally benign proline-catalyzed multi-component synthesis of novel octahydropyrimido[4,5-*g*]quinazolin-5,10-diones has been developed, using ethanol as green solvent and L-proline as green organocatalyst. Products were generally isolated via simple filtration. This reaction proved highly suitable for electron rich anilines, however, unsuccessful for electron-withdrawing substituents on aniline and primary alkylamines. These *p*-quinone derivatives, octahydropyrimido[4,5-*g*]quinazolin-5,10-diones, showed a strong tendency to form SAMNs on a graphitic surface, which was observed for analogues with different alkyl chain lengths and different aniline derivatives. The aniline groups were observed to take an edge-on orientation with respect to the graphite surface to maximize π - π interactions between adjacent aniline groups. Additionally, the presence of substituted aniline groups was observed to be key to the formation of a SAMN. The molecular characteristics can easily be altered to change the type of SAMN that is formed on the HOPG surface. The redox behavior was studied by cyclic voltammetry in DMF.

Acknowledgements

W.D. and S.D.F. acknowledge financial support for this work by KU Leuven (C14/19/078 and C14/19/079). S. D. F. acknowledges support from Research Foundation – Flanders (FWO) (GF9118N). The authors thank Bart Van Huffel for technical assistance with NMR spectrometry and Jef Rozenski for HRMS measurements. B.D. thanks Kunal Mali and Roelof Steeno for their help in analyzing the STM images. Mass spectrometry was made possible by the support of the Hercules Foundation of the Flemish Government (grant 20100225-7). L.V.M. thanks the Hercules Foundation for supporting the purchase of the diffractometer through project AKUL/09/ 0035.

Conflicts of interest

There are no conflicts to declare

References

- 1 A. M. Weyers, R. Chatterjee, S. Milikisiyants and K. V. Lakshmi, *J. Phys. Chem. B*, 2009, **113**, 15409–15418.
- 2 J. Gutiérrez-Fernández, K. Kaszuba, G. S. Minhas, R. Baradaran, M. Tambalo, D. T. Gallagher and L. A. Sazanov, *Nat. Commun.*, 2020, **11**, 4135.
- 3 C. E. Pereyra, R. F. Dantas, S. B. Ferreira, L. P. Gomes and F. P. Silva-Jr, *Cancer Cell Int.*, 2019, **19**, 207.
- 4 K. W. Wellington, N. I. Kolesnikova, N. B. P. Nyoka and L. J. McGaw, *Drug Dev. Res.*, 2019, **80**, 138–146.
- 5 J. Campanini-Salinas, J. Andrades-Lagos, G. Gonzalez Rocha, D. Choquesillo-Lazarte, S. Bollo Dragnic, M. Faúndez, P. Alarcón, F. Silva, R. Vidal, E. Salas-Huenuleo, M. Kogan, J. Mella, G. Recabarren Gajardo and D. Vásquez-Velásquez, *Mol.*, 2018, **23**.
- 6 O. P. S. Patel, R. M. Beteck and L. J. Legoabe, *Eur. J. Med. Chem.*, 2021, **210**, 113084.
- 7 E. J. Son, J. H. Kim, K. Kim and C. B. Park, *J. Mater. Chem. A*,

- 2016, **4**, 11179–11202.
- 8 M. Lee, J. Hong, H. Kim, H.-D. Lim, S. B. Cho, K. Kang and C. B. Park, *Adv. Mater. (Weinheim, Ger.)*, 2014, **26**, 2558–2565.
- 9 K. S. Mali, J. Adisojoso, E. Ghijsens, I. De Cat and S. De Feyter, *Acc. Chem. Res.*, 2012, **45**, 1309–1320.
- 10 K. S. Mali, J. Adisojoso, I. De Cat, T. Balandina, E. Ghijsens, Z. Guo, M. Li, M. S. Pillai, W. Vanderlinden, H. Xu and S. De Feyter, in *Supramolecular Chemistry: From Molecules to Nanomaterials*, John Wiley & Sons Ltd., 2012, p. 3419.
- 11 Y. Fang, M. Cibian, G. S. Hanan, D. F. Perepichka, S. De Feyter, L. A. Cuccia and O. Ivashenko, *Nanoscale*, 2018, **10**, 14993–15002.
- 12 Y. Fang, Concordia University, 2013.
- 13 H. Möhrle and G. S. Herbrüggen, *Arch. Pharm. (Weinheim)*, 1991, **324**, 165–171.
- 14 S. OHTA, Y. HINATA, M. YAMASHITA, I. KAWASAKI, Y. JINDA and S. HORIE, *Chem. Pharm. Bull. (Tokyo)*, 1994, **42**, 1730–1735.
- 15 M. I. P. Reis, V. R. Campos, J. A. L. C. Resende, F. C. Silva and V. F. Ferreira, *Beilstein J. Org. Chem.*, 2015, **11**, 1235–1240.
- 16 A. Alekszi-Kaszas, P. Nemes, G. Toth, J. Halasz and P. Scheiber, *Synth. Commun.*, 2018, **48**, 2099–2111.
- 17 F.-L. Zhao and J.-T. Liu, *J. Fluor. Chem.*, 2004, **125**, 1491–1496.
- 18 K. Chanda, M. C. Dutta, E. Karim and J. N. Vishwakarma, *J. Heterocycl. Chem.*, 2004, **41**, 627–631.
- 19 Y. Lin, J.-T. Liu and F.-L. Zhao, *J. Fluor. Chem.*, 2005, **126**, 1539–1542.
- 20 Z.-P. Chen, H.-B. Wang, Y.-Q. Wang, Q.-H. Zhu, Y. Xie and S.-W. Liu, *Tetrahedron*, 2014, **70**, 4379–4385.
- 21 E. M. Afsah, E.-S. I. El-Desoky, H. A. Etman, I. Youssef and A. M. Soliman, *J. Heterocycl. Chem.*, 2018, **55**, 2959–2970.
- 22 C. Hansch, A. Leo and R. W. Taft, *Chem. Rev.*, 1991, **91**, 165–195.
- 23 S. Sergeev, *Helv. Chim. Acta*, 2009, **92**, 415–444.
- 24 T. Habets, D. Lensen, S. Speller and J. A. A. W. Elemans, *Molecules*, 2019, **24**, 3018.
- 25 A. Gesquiere, M. M. S. Abdel-Mottaleb, S. De Feyter, F. C. De Schryver, F. Schoonbeek, J. van Esch, R. M. Kellogg, B. L. Feringa, A. Calderone, R. Lazzaroni and J. L. Bredas, *Langmuir*, 2000, **16**, 10385–10391.
- 26 S. A. Arnstein and C. D. Sherrill, *Phys. Chem. Chem. Phys.*, 2008, **10**, 2646–2655.
- 27 M. O. Sinnokrot and C. D. Sherrill, *J. Phys. Chem. A*, 2003, **107**, 8377–8379.
- 28 J. Q. Chambers, *Quinonoid Compd.*, 1988, 719–757.
- 29 P. S. Guin, S. Das and P. C. Mandal, *Int. J. Electrochem.*, 2011, 816202.
- 30 M. O. F. Goulart, N. M. F. Lima, A. E. G. Sant’Ana, P. A. L. Ferraz, J. C. M. Cavalcanti, P. Falkowski, T. Ossowski and A. Liwo, *J. Electroanal. Chem.*, 2004, **566**, 25–29.